AJNR

Proton MR spectroscopy and magnetization transfer ratio in multiple sclerosis: correlative findings of active versus irreversible plaque disease.

H Kimura, R I Grossman, R E Lenkinski and F Gonzalez-Scarano

This information is current as of April 17, 2024.

Proton MR Spectroscopy and Magnetization Transfer Ratio in Multiple Sclerosis: Correlative Findings of Active versus Irreversible Plaque Disease

Hirohiko Kimura, Robert I. Grossman, Robert E. Lenkinski, and Francisco Gonzalez-Scarano

PURPOSE: To characterize plaques of multiple sclerosis (MS) using both proton MR spectroscopy and magnetization transfer (MT) imaging. **METHODS:** The magnetization transfer ratio (MTR) was calculated from two series of three-dimensional gradient-recalled acquisition in the steady state (GRASS) images obtained with and without an MT saturation pulse. Proton spectra were acquired using the point-resolved spectroscopy (PRESS) sequence with a voxel size of $1.5 \times 1.5 \times 1.5 \ cm^3$. A total of 28 spectra were obtained in 13 patients who had clinically definitive MS. The spectra were analyzed together with the MTR. **RESULTS:** A positive relationship was found between the *N*-acetylaspartate (NAA)/creatine (Cr) ratio and the MTR in MS plaques, whereas no significant correlation was found between the metabolite ratios and the signal intensity on fast spin-echo T2-weighted MR images. **CONCLUSION:** Small changes in the MTR of MS plaques relative to the MTR of normal white matter may reflect inflammatory changes and edema, whereas larger changes in MTR correlate with decreased NAA/Cr ratio and therefore suggest demyelination and irreversible damage from chronic MS plaques.

Index terms: Magnetic resonance, magnetization transfer; Magnetic resonance, spectroscopy; Sclerosis, multiple

Multiple sclerosis (MS) is a relapsing-remitting disease in the central nervous system that forms plaques in various stages of the demyelinating process. Magnetic resonance (MR) imaging has been used extensively as one of the diagnostic procedures to demonstrate MS plaques. Although MR imaging has excellent sensitivity in detecting the lesions, it still lacks the specificity for characterizing the precise stage of the demyelinating process.

Magnetization transfer (MT) imaging is a relatively new technique that modifies the image contrast by means of selective saturation of restricted protons in macromolecules and associated water protons (1, 2). In previous studies, the measurement of magnetization transfer ratio (MTR) has proved useful for the differentiation of primarily demyelinating lesions from those that are mainly edematous in MS plaques (3). MT imaging also has the advantage of being able to detect wallerian degeneration in visual pathways (4). It is clear that the MTR reflects changes in the amount and type of macromolecules present in white matter. Therefore, MT imaging may provide a method for the assessment of myelin integrity.

Like MR imaging, proton MR spectroscopy has shown potential in diagnosing MS and in monitoring the progression of treatment (5). In addition, it provides further characterization of MS plaques that is based on the biochemical composition of the plaque volume. Proton MR spectroscopy along with MR imaging may be helpful for differentiating those early lesions from late irreversible gliotic lesions (6). Because *N*-acetylaspartate (NAA) is thought to be specifically located in neurons in gray matter

and in axonal processes in white matter (7, 8), there is an emerging consensus that the level of NAA detected with proton MR spectroscopy is an index of neuronal viability in brain tissue.

We hypothesized that the combined use of MT imaging and MR spectroscopy may provide information about the relationship between myelin damage and the metabolite changes detected by proton MR spectroscopy and thus provide a means for staging plaques. To test this thesis, we measured both the MTR and the NAA/creatine (Cr) ratio from the same brain region in order to determine whether myelin damage detected with MT imaging correlates with neuronal loss detected with MR spectroscopy.

Subjects and Methods

Thirteen patients (nine women and four men, 23 to 50 years old) with clinically definitive MS were studied with both MT imaging and MR spectroscopy. The known duration of the disease varied from 2 to 21 years. All the MT imaging and MR spectroscopy studies were performed after informed consent was obtained from patients. Twenty studies were obtained from the 13 patients. Seven patients had follow-up examinations 5 to 7 months after the first examination. In all seven of these patients the location of MR spectroscopy voxels was different on the original and the follow-up examinations. Two separate locations were assessed in eight of 20 examinations, and, in total, 28 proton spectra were analyzed along with the MTR measurements. The analysis and the selection of the regions of interest (ROIs) were done by the same observer.

Twelve healthy control subjects (27 to 43 years old) were examined with MR spectroscopy and six control subjects (28 to 45 years old) were examined with MT imaging. In the MR spectroscopy group, one location was studied for each subject; in the MT imaging group, two locations were studied for each of the six subjects.

All MT imaging and MR spectroscopy studies were performed on a 1.5-T MR imager. The MR imaging protocol consisted of sagittal T1-weighted 600/17/1 (repetition time/echo time/excitations) sequences with a 5-mm section thickness and a 256×192 matrix; axial fast spin-echo T2-weighted 2700/17,85/1 sequences with a 3-mm section thickness and a 256×192 matrix; and axial three-dimensional gradient-recalled acquisition in the steady state (GRASS) images, 106/5/1, with a 5-mm section thickness, a $256 \times 128 \times 28$ matrix, and a 12° flip angle. The last images were obtained with and without an MT saturation pulse during the same series, holding all prescan parameters constant. MT saturation was achieved by a prolonged, off-resonance, preexcitation radio frequency pulse (19-millisecond single-cycle sinc-shaped, 2 KHz off-resonance from water, averaged B_1 intensity 3.67×10^{-6} T) (9). The formula used for the calculation of MTR was as follows: $(MT_0 - MT_{sat})/MT_0 \times 100\%$, where MT_0 is signal intensity before the MT pulse has been applied, and MT_{sat} is signal intensity after the MT pulse has been applied. MTR map images were constructed from the two sets of 3-D GRASS images with and without an MT saturation pulse. Image data were transferred to a workstation for computation of pixel-by-pixel MTR maps. Misregistration between the two series of images was corrected by shifting appropriate numbers of pixels in each image on the computer screen interactively, as necessary. The mean value of the MTR was obtained simply by averaging pixel values in the ROI on the MTR map. To demonstrate the distribution of abnormal MTR pixels on the MTR map, we calculated subtraction MTR images, on which the pixels with lower MTR values were replaced with the value of 0, so that abnormal pixels could be seen as areas of signal void.

Water-suppressed localized proton MR spectroscopy studies were acquired by using the PRESS sequence with a solvent suppression scheme in the preparation period. Water suppression was achieved by three repeated chemical selective saturation pulses (50-Hz bandwidth), each followed by a dephasing gradient. A spectrum was obtained from the voxel of $1.5 \times 1.5 \times 1.5$ cm^3 using the following parameters: 2000/25/256, 1250-Hz sweep width, 2048 data points, and an eight-step phase cycle. Postacquisitional water suppression was performed by subtracting the low-frequency component from the original free-induction decay in the time domain data, if needed, to avoid baseline elevation toward the residual water peak (10). Data processing included zero filling to 4K data points, 1-Hz exponential line broadening, Fourier transformation, and zero-order phase correction. Peak areas were determined by Lorentian curve fitting.

To compare the metabolite ratios and the MTR from the same brain tissue, we analyzed two adjacent sections on the MT images that nominally covered 1 cm of a 1.5-cm MR spectroscopy voxel in the section direction. The relative percentages of pixels with diminished MTR values within the MR spectroscopy voxels were calculated: (the number of pixels with diminished MTR)/(the total number of pixels in MR spectroscopy voxels) $\times$ 100. These values were compared with those from control white matter. To ascertain the partial volume effect of white matter surrounding the MS plaque in the MR spectroscopy voxel, we measured the mean MTR values in the central part of the MS plaques seen in the MR spectroscopy voxels (a round ROI with a 5-mm diameter in each image) as well as the MTR values for the whole MR spectroscopy voxels. Signal intensity on T2-weighted images was also measured after normalizing the signal intensity of cerebrospinal fluid (CSF) to 100. The mean signal intensity on T2-weighted MR images of corresponding whole MR spectroscopy voxels was compared with those obtained from MTR maps. To correlate the metabolite ratios and the signal intensity from the same brain region, we used three sections on T2-weighted images that again nominally covered 9 mm of a 1.5-cm MR spectroscopy voxel in the section direction. We assumed that the threshold level of high signal intensity for MS plaques was 55% of CSF intensity on T2-weighted

images, because this level can be confidently recognized as high-signal-intensity lesions on visual inspection of T2-weighted images. Using this plaque intensity threshold, we calculated the percentage of volume of MS plaques relative to the whole MR spectroscopy voxel: (the number of pixels with higher than normalized 55% value)/(the total number of pixels in the MR spectroscopy voxel) $\times$ 100. This value was used as validation that MS plaques occupied a large enough volume to compare metabolite ratios obtained from a given MR spectroscopy voxel.

To categorize lesions with the same type of disease, we classified lesions into three groups depending on their appearance on T2-weighted images at the site of the MR spectroscopy voxel: group 1 was normal-appearing white matter (n = 5); group 2, diffuse hyperintense lesions (n = 4); and group 3, focal lesions of high intensity (n = 19). Normal-appearing white matter was defined as white matter without abnormal high signal in MR spectroscopy voxels on T2-weighted images; diffuse hyperintensity lesions were those that showed diffuse high signal extending throughout the MR spectroscopy voxel; and focal lesions of high intensity were patchy plaquelike foci of high signal intensity confined inside the MR spectroscopy voxel. The metabolite ratios and the MTR in each group were compared with those obtained from the MR spectroscopy and MT imaging control groups using an unpaired t test. For the linear correlative analysis between the NAA/Cr and the MTR in the group of focal lesions of high intensity, we excluded five small MS plaques that occupied a limited volume in the MR spectroscopy voxel (fewer than 50% of pixels) to minimize partial volume effects from surrounding normal-appearing white matter. In total, 14 spectra along with the value of the MTR were analyzed in the test of linear regression parameters. The corresponding signal intensity on T2-weighted images was also correlated with the ratio of NAA/Cr.

Results

Control White Matter

A proton spectrum of white matter of a healthy volunteer (a 31-year-old man) is shown in Figure 1 for comparison. Resonances in proton spectra of brain tissue are assigned to NAA (methyl singlet at 2.01 ppm); coupled multiplets of glutamate and glutamine (Glx, at 2.1 to 2.4 ppm); creatine and phosphocreatine (Cr, at 3.02 ppm); choline-containing compounds (Cho, at 3.20 ppm); and *myo*-inositol (Ins, at 3.56 ppm). The results of quantitative analysis of proton spectra from healthy control subjects are summarized in Table 1 as metabolite area ratios. Figure 2 shows the control T2-weighted images at the level of the lateral ventricle and the MTR map images of the same brain sections.
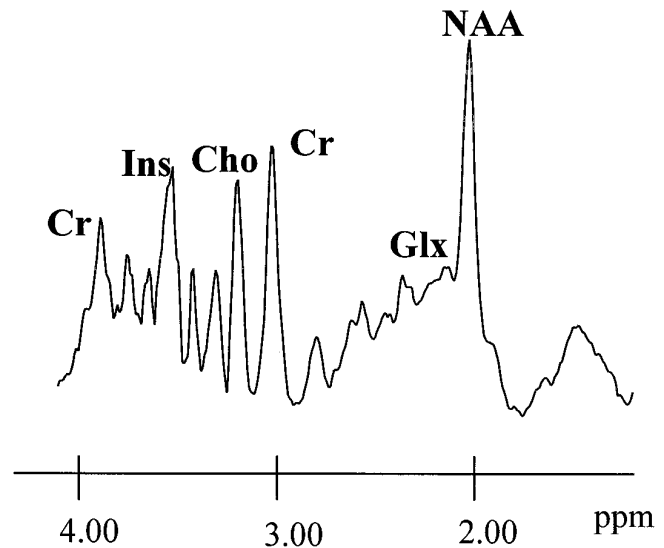

Fig 1. A proton MR spectrum (2000/25) obtained from the white matter of a 31-year-old healthy control subject. A 15 $\times$ 15 $\times$ 15-mm^3 (3.4-mL) volume of interest was located at the centrum semiovale level of the brain. *NAA* indicates *N*-acetylaspartate; *Cr*, creatine and phosphocreatine; *Cho*, choline-containing compounds; *Ins*, *myo*-inositol; and *Glx*, glutamate and glutamine. The chemical shift in parts per million (*ppm*) is referenced to the methyl peak of NAA as 2.01 ppm.

Normal-Appearing White Matter

The metabolite ratios obtained by MR spectroscopy revealed no significant difference from those of healthy control subjects (Table 1). Although the average value of the MTR in the MR spectroscopy voxel showed no significant difference from that of the control value, the number of pixels with a decreased MTR was slightly increased (Table 2). In fact, the pixels with decreased MTR values appeared to be scattered more frequently throughout the white matter on the MTR maps of one patient in this group (Fig 3).

Diffuse High-Signal-Intensity Lesions

Figure 4 shows a proton MR spectrum from a 3.4-mL volume of white matter in one patient in this group (a 34-year-old woman). A prominent Cho peak was seen in this spectrum, whereas the NAA peak appeared to be of normal height as compared with the normal control spectrum in Figure 1. T2-weighted images in this patient showed the diffuse high signal intensity and small bright plaques scattered inside the MR spectroscopy voxel (Figure 5, top row) whereas the subtraction MTR map images clearly showed the small areas of signal void in the

TABLE 1: In vivo metabolite ratios in patients with multiple sclerosis and healthy control subjects

	NAA/Cr	Cho/Cr	NAA/Cho
Control white matter (n = 12)	1.67 ± 0.24	0.96 ± 0.17	1.77 ± 0.33
Normal-appearing white matter (n = 5)	1.46 ± 0.27	0.82 ± 0.06	1.81 ± 0.46
	(NS)	(NS)	(NS)
Diffuse hyperintensity lesions (n = 4)	1.58 ± 0.41	1.23 ± 0.28	1.35 ± 0.46
	(NS)	(NS)	(NS)
Focal lesions of high intensity (n = 19)	1.28 ± 0.33	1.07 ± 0.23	1.26 ± 0.42
	($P < .05$)	(NS)	($P < .05$)

Note.—All values are expressed as mean ± SD; statistical significance was determined with unpaired Student's t test between control white matter values and each group of multiple sclerosis. NS indicates not significant.

Fig 2. Fast spin-echo T2-weighted (2000/80) MR images (*top row*) and subtraction MTR maps (>37.5%) (*bottom row*) of normal control white matter sectioned nominally at the same brain level. No abnormal white matter signal is seen on the MR images, and only several signal voids can be observed in the white matter on the MTR maps.
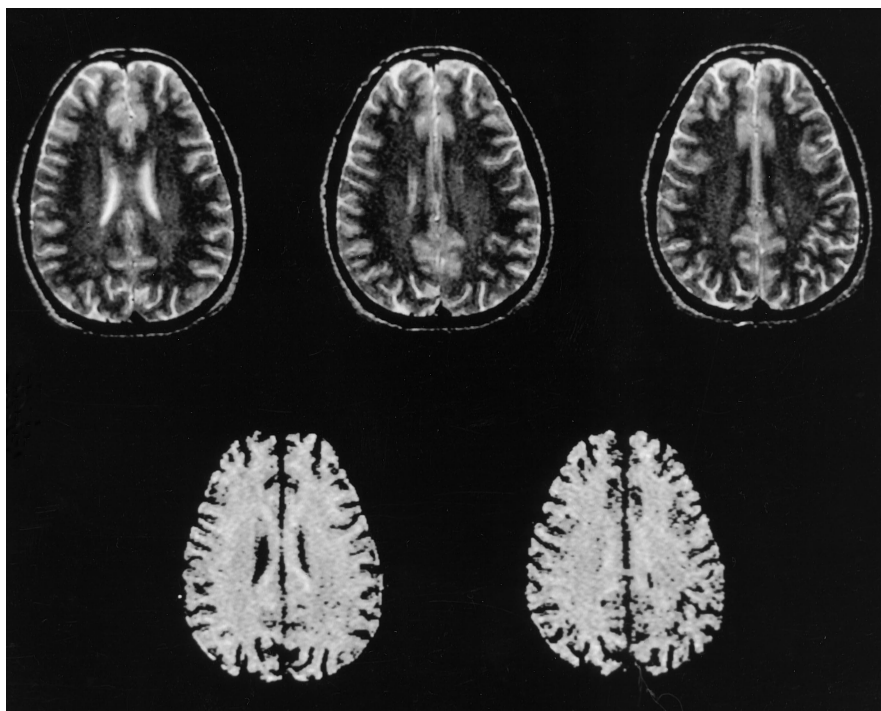
corresponding region (Fig 5, bottom row). The metabolite pattern in this group showed high Cho/Cr ratios compared with control values using an unpaired t test ($P < .05$). There was no statistical difference between the NAA/Cr ratio and that of the control group (Table 1). The relative volumes with decreased MTR showed a slight but statistically significant increase ($P < .05$), whereas the signal intensity on T2-weighted images was significantly increased ($P < .0005$) compared with that of control subjects.

Focal Lesions of High Intensity

Figure 6 shows typical proton spectra from an MS plaque in temporoparietal white matter in a 36-year-old man. Decreased levels of NAA and relatively high levels of Cho are seen. No resonances from lactate or mobile lipids were seen in this lesion (lactate doublets, 1.32 ppm with 7-Hz splitting; broad lipid peaks, 1.2 to 1.3 and 0.8 to 0.9 ppm). High signal intensity scattered throughout the periventricular white matter on T2-weighted images was observed (Fig 7, top row), and abnormal pixels occupied almost all parts of the MR spectroscopy voxel on the MTR maps (Fig 7, bottom row). Both the NAA/Cr and NAA/Cho ratios were significantly decreased in these lesions compared with control ratios; however, the Cho/Cr peak did not differ statistically from that of control subjects, although an increasing trend was observed in some patients (Table 2). Measurements of MTR

TABLE 2: Magnetization transfer ratio (MTR) and signal intensity on T2-weighted MR images

	Averaged MTR in MR Spectroscopy Voxels*	Percentage of Pixels with MTR Less Than 37.5†	Percentage of Pixels with MTR Less Than 35.0†	Signal Intensity on T2-Weighted Images‡
Control white matter (n = 12)	41.9 ± 1.1	4 ± 5	1 ± 1	44.0 ± 1.8
Normal-appearing white matter (n = 5)	40.9 ± 1.0 (NS)	10 ± 1 ($P < .05$)	2 ± 1 ($P < .05$)	44.5 ± 2.6 (NS)
Diffuse hyperintensity lesions (n = 4)	40.8 ± 0.6 (NS)	11 ± 6 ($P < .05$)	3 ± 2 ($P < .005$)	52.1 ± 1.4 ($P < .0005$)
Focal lesions of high intensity (n = 19)	35.7 ± 3.0 ($P < .0005$)	43 ± 26 ($P < .0005$)	30 ± 25 ($P < .0005$)	61.3 ± 7.9 ($P < .0005$)

Note.—All values are expressed as mean ± SD; statistical significance was determined with unpaired Student's t test between control white matter values and each group of multiple sclerosis. NS indicates not significant.

* Including multiple sclerosis plaques.

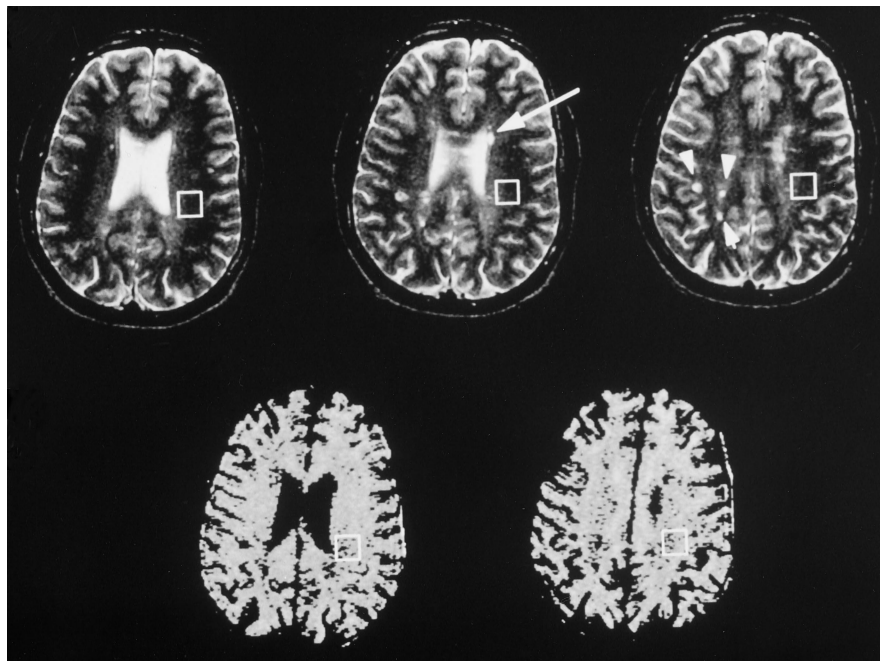† In MRS voxels.

‡ Normalized to CSF intensity (CSF = 100).

Fig 3. Fast spin-echo T2-weighted (2000/80) MR images (*top row*) and subtraction MTR maps (>37.5%) (*bottom row*) of normal-appearing white matter sectioned nominally at the same brain level. Small MS plaques can be seen as bright signal areas in the right parietooccipital region (*arrowheads*) and adjacent to the anterior aspect of the left lateral ventricle (*arrow*) on the MR images. No definitive abnormal signal intensity is seen in the MR spectroscopy voxels in the white matter of T2-weighted images. Scattered areas of signal voids can be seen in the white matter on the MTR maps more frequently than the apparent bright plaques on the MR images. *Black* within the MR spectroscopy voxel denotes that the pixel value of the MTR was less than 37.5%.

in MR spectroscopy voxels revealed an apparent decrease of MTR values. The large fraction of pixels inside the MR spectroscopy voxel had a value of less than 35% (Table 2). The central part of the MS plaques showed lower MTR values than those obtained from whole MRS voxels (31.5% ± 3.6%; see Table 2). Figure 8 shows the scatter plots of NAA/Cr ratios against the MTR or T2 intensity obtained from MS plaques. A positive linear relationship was found between the MTR and the averaged NAA/Cr ratio in the white matter–containing MS plaques. A positive linear relationship was also observed between the NAA/Cr ratio and the MTR values from the central part of the plaques ($r = .55$, $P < .05$). No significant correlation was found between the
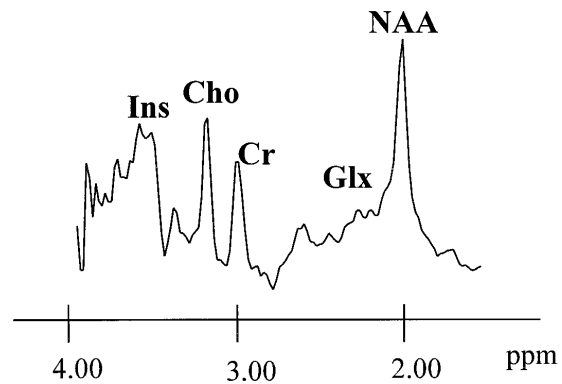

Fig 4. A proton MR spectrum (25/2000) obtained from the white matter of a 34-year-old patient with MS. A 15 × 15 × 15-mm³ (3.4-mL) volume of interest was located in the left temporooccipital white matter of brain (see Fig 6). The high Cho peak is characteristic of the spectra from this group of patients. (See legend to Figure 1 for definition of abbreviations.)

Fig 5. T2-weighted MR images (*top row*) and MTR maps (*bottom row*) of a diffuse hyperintensity lesion. Diffuse high signal intensity and focal brighter area (*arrowhead*) are visible on MR images inside the MR spectroscopy voxel. Subtraction MTR maps show the small area of signal voids in the MR spectroscopy voxel (MTR <37.5%).
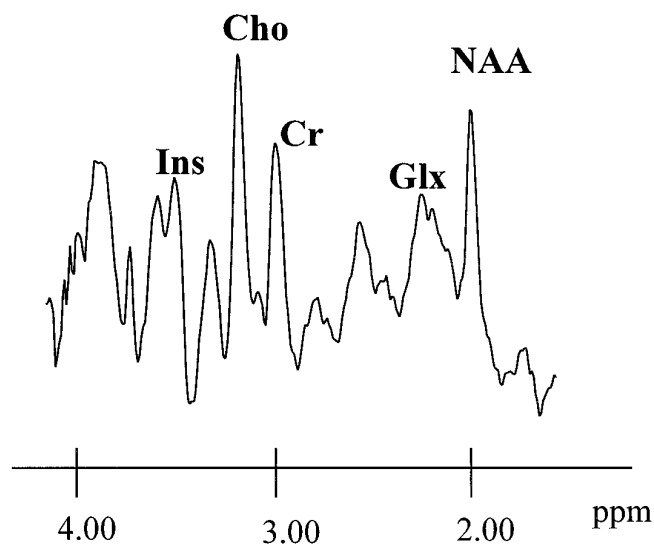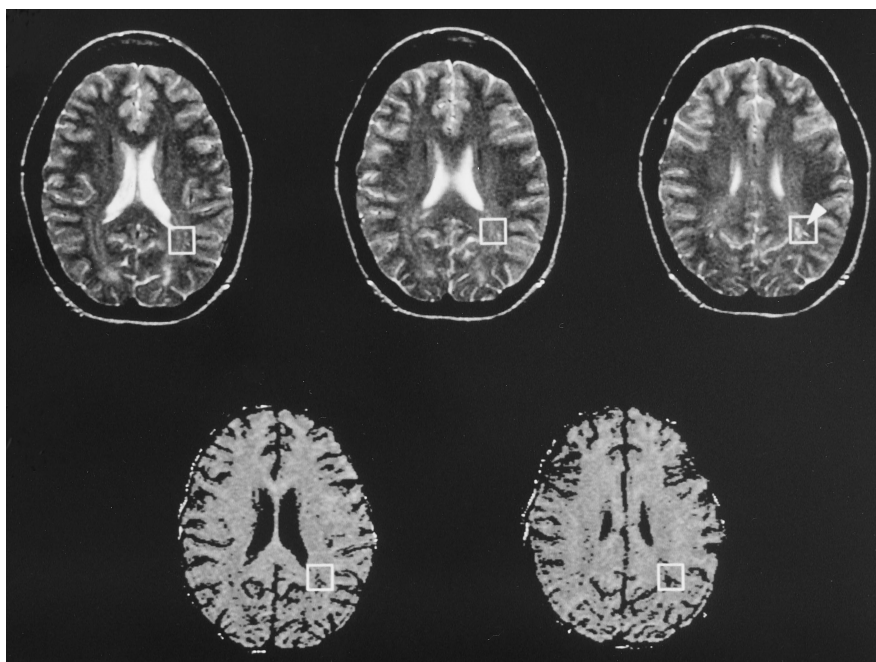

Fig 6. A proton MR spectrum obtained from an MS plaque in a 36-year-old patient. Localized voxel is drawn on localizing images for MR spectroscopy (see Fig 7). Diminished NAA and elevated Cho peak are apparent, as compared with control spectrum (Fig 1). (See legend to Figure 1 for definition of abbreviations.)

metabolite ratios and the signal intensity on T2-weighted images (Fig 9).

Discussion

In MS, the most specific and characteristic change is demyelination. However, it is likely that each plaque consists of different and heterogeneous stages in this process. Thus, char-

acterizing individual MS lesions is of critical importance not only in understanding MS but also in planning treatment. Some MS lesions are purely edematous or inflammatory in nature and should respond to steroid therapy (11). Other chronic lesions that are replaced by astrocytic gliosis most likely will not respond to any current medical treatment. Therefore, the differentiation of edematous lesions from highly demyelinated or gliotic lesions would be important to both patients and their physicians. Many of the spectroscopic studies performed in MS have addressed this point. The hypothesis is that metabolite ratios are unchanged in hyperacute (edema only) plaques. Demyelination in acute plaques is accompanied by an increased Cho/Cr ratio (12, 13). Irreversible plaques in chronic stages have decreased NAA/Cr ratios (6, 14). Some investigators have proposed increased lipid peaks (15–17) or increased lactate resonances (12, 13) as early indications of active MS plaques. Others have reported that the increased ratio of amino acid to creatine (AA/Cr) is observed as myelin is degraded in an active stage of the plaques, especially in contrast-enhanced plaques (18). Because NAA is found almost exclusively in neuronal cells (7, 8, 19), the reduction of the NAA/Cr ratio in MS plaques has been considered to be a reflection of cumulative irreversible tissue damage and, hence, neuronal dysfunction or the loss of neu-
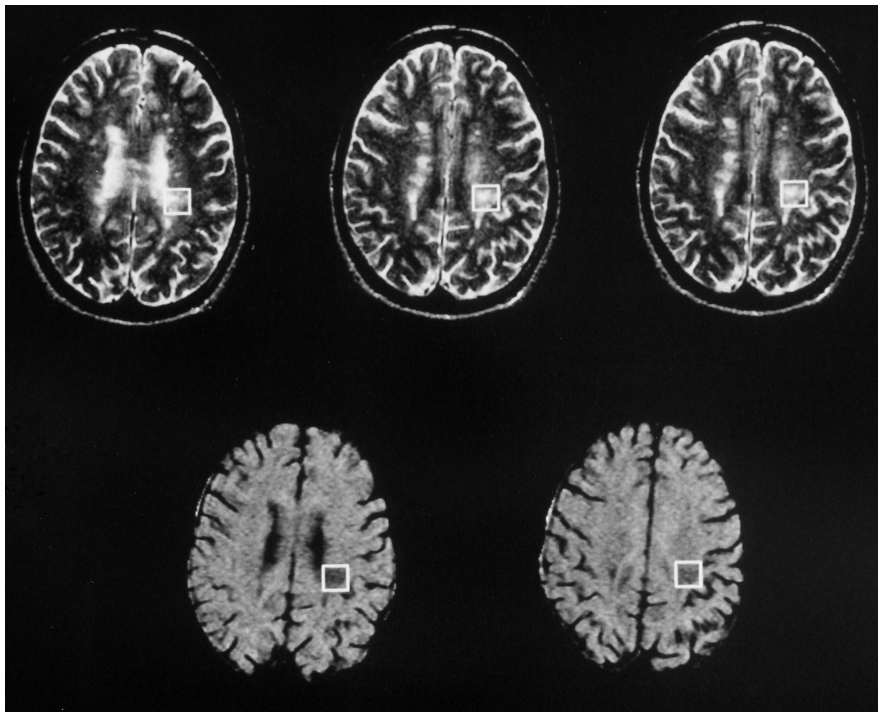
Fig 7. T2-weighted MR images (*top row*) and MTR maps (*bottom row*) in a 36-year-old patient with MS. A 1.5-cm volume of interest was located in the left paraventricular white matter in the temporoparietal region. Averaged signal intensity of the MR spectroscopy voxel is 68% relative to CSF intensity (CSF = 100), while the averaged MTR of the same voxel is 31%. A major part of the MR spectroscopy voxel (77%) exhibits decreased intensity on the MTR map (MTR values are less than 37.5%).
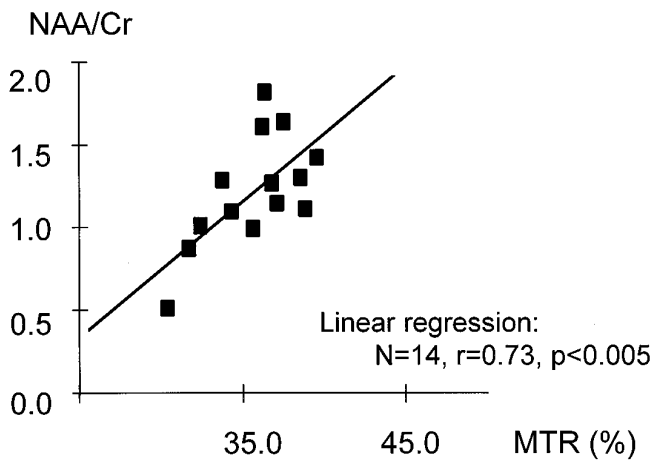

Fig 8. Two-dimensional plots of NAA/Cr ratio versus MTR of voxels containing MS plaques. There is a significant linear relationship between the NAA/Cr ratio and the MTR.
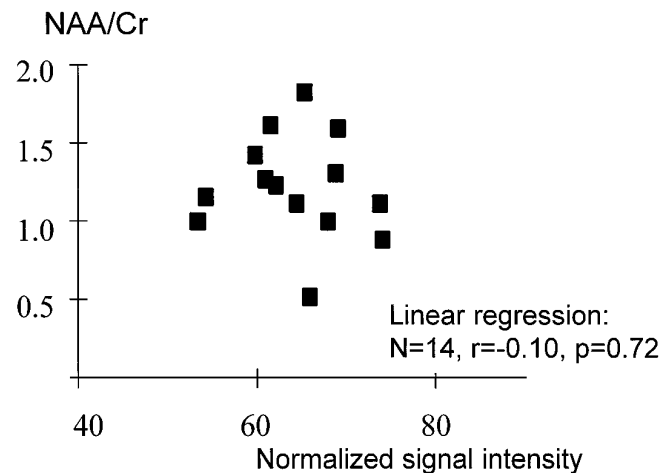

Fig 9. Two-dimensional plots of NAA/Cr ratio versus signal intensity of MS plaques on T2-weighted MR images. No significant linear relationship was found between the NAA/Cr ratio and signal intensity on T2-weighted images.

rons in the chronic phase of a demyelinating process.

The availability of MT has provided new insight into the status of macromolecules in the tissue. The exchange of magnetization between free water and bound water surrounding the macromolecules will affect imaging contrast (1, 2). The main source of these macromolecules in white matter is myelin. Therefore, the loss of myelin will directly cause a reduction of the bound water pool, which will lead to a decrease in the MT effect. In a previous study, the wide range of MTR values in MS lesions was attributed to the difference in the stages of demyelination, and consequently, to differences in the age of the plaque (3). Again, the reduction of MTR is consistent with the demyelinated state of plaques.

In this study, spectra obtained from normal-appearing white matter were indistinguishable

from those obtained in healthy control subjects. A previous study has demonstrated a significant difference between the MTR in the normal-appearing white matter of MS patients and that of healthy control subjects (20). In the current comparison, the mean value of the MTR was within the range of normal, probably because of the averaging of pixels with the mostly normal MTR value in the large MR spectroscopy voxel. However, the pixels with decreased MTR values appeared to be more scattered than those of control white matter on MTR map images. In this regard, our result was consistent with the previous reports (3, 20). By far the most common microscopic abnormality was gliosis in macroscopically normal white matter in MS patients (21). Therefore, the foci of reduced MTR shown on the subtraction MTR maps might correspond to microscopic lesions distributed in normal-appearing white matter, in which the myelin content is relatively reduced as a result of gliotic change.

Diffuse hyperintensity lesions also contained scattered pixels with reduced MTR as well as diffusely increased intensity on T2-weighted images. Note that a large fraction of pixels in the voxel still have a normal MTR value despite the definitive high signal intensity on T2-weighted images. Although the pixels with diminished MTR may be considered the demyelinated portion in the MR spectroscopy voxel, the majority of pixels within MR spectroscopy voxels probably had simple edematous change not accompanied by definitive myelin change. This is also in accordance with the normal value of the NAA/Cr ratio and the high Cho/Cr ratio in this group, since the former ratio from MS plaques remains unchanged and the latter ratio is high in the acute phase of MS plaques, as reported previously (12, 13, 22). Thus, if the lesions in this group are in the acute stage with edema, the metabolite change is consistent with the MTR values in the MR spectroscopy voxel and with the hyperintensity seen on T2-weighted images.

The NAA/Cr ratio of focal lesions was significantly decreased from that of the control group, whereas the Cho/Cr ratio revealed no significant difference from that of the control group. The reduction of the NAA/Cr ratio in MS plaques has been attributed to the loss of neuronal cells (6, 13). On the other hand, the increased Cho/Cr ratio has been discussed in relation to the degradation process of cells (12, 13), since this

peak may contain catabolic products of membrane metabolism, such as glycerophosphocholine. Therefore, the change in the Cho/Cr ratio may be dependent on the stage of activity of this process. The plaque with the lowered NAA/Cr ratio and the normal Cho/Cr ratio might be considered a chronic plaque with no inflammatory activity.

In this correlative study of focal plaque lesions, we have shown a positive correlation between the MTR and the NAA/Cr ratio, which supports the concept that the MT image is sensitive to the presence of real myelin damage, and that those lesions with lowered MTR ultimately evolve into an irreversible stage in the degeneration and gliosis of neuronal tissue. These plaques will also have lowered NAA/Cr ratios on proton MR spectroscopy. Although both the MTR and the NAA/Cr ratio changed along with the plaque age, the alteration of MTR may occur at an earlier stage of the demyelinating process, since a recent study has shown the positive inverse correlation between MTR and AA/Cr (23). On the other hand, the NAA/Cr ratio was not well correlated with the regional intensity of the plaque on T2-weighted images. The signal intensity of T2-weighted images is not specific to the type of MS plaque, whether edema, demyelination, or gliosis, whereas the NAA/Cr ratio may be dependent on the neuronal density left in the plaque. This is one possible explanation as to why a lack of correlation was found between the intensity on T2-weighted images and the NAA/Cr ratio.

The results of the correlative study for the group of focal lesions of high intensity should be interpreted carefully, because MR spectroscopy data from a 1.5-cm voxel will still have considerable partial volume effects of normal-appearing white matter surrounding MS plaques. However, we note that the positive linear relationship was also observed between the MTR in the central part of the plaques and the NAA/Cr ratio. Since the mean MTR from the central part of the plaques was calculated from constant volume in MS plaques, this MTR value was not affected by the MTR value from surrounding white matter. Therefore, the MTR from the plaque itself plays a certain role in the correlation of metabolite ratios, although some partial volume effects are unavoidable under the current resolution of MR spectroscopy studies.

Again, the correlation between the NAA/Cr ratio and the MTR is very important. Lesions

with a low MTR correlate with the finding of a low NAA/Cr ratio; therefore, they may prove to be markers of irreversible damage, because a low NAA/Cr ratio has been considered to be a sign of irreversible neuronal damage in MS plaques. If this is true, the region with a decreased MTR will probably lose its neuronal integrity or neuronal tissue in time, although serial or longitudinal studies are required to validate this. However, it is likely that a small reduction in the MTR seen in simple edematous MS lesions may be reversible to a normal MTR range, since the small decrease in the MTR seen in a model of experimental allergic encephalomyelitis has been attributed to the relative dilution of macromolecular concentration and not to real myelin damage (3). Another potential significance of the current result is that, for certain studies, MT imaging may be able to substitute partly for proton MR spectroscopy, which will enable the characterization of MS plaques in the whole brain with greater spatial resolution and in less examination time.

In summary, our results suggest that the diminished MTR detected in MS lesions may be a marker for irreversible cell damage, as evidenced by the decreased NAA/Cr ratio observed in the MR spectroscopy study.

References

1. Balaban RS, Ceckler TL. Magnetization transfer contrast in magnetic resonance imaging. *Magn Reson Q* 1992;8:116–137
2. Wolff SD, Balaban RS. Magnetization transfer contrast (MTC) and tissue water proton relaxation in vivo. *Magn Reson Med* 1989;10:135–144
3. Dousset V, Grossman RI, Ramer KN, et al. Experimental allergic encephalomyelitis and multiple sclerosis: lesion characterization with magnetization transfer imaging. *Radiology* 1992;182:483–491
4. Lexa FJ, Grossman RI, Rosenquist AC. MR of wallerian degeneration in the feline visual system: characterization by magnetization transfer rate with histopathologic correlation. *AJNR Am J Neuroradiol* 1994;15:201–212
5. Richards T. Proton MR spectroscopy in multiple sclerosis: value in establishing diagnosis, monitoring progression, and evaluating therapy. *AJR Am J Roentgenol* 1991;157:1073–1078
6. Arnold D, Matthews P, Francis G, Antel J. Proton magnetic resonance spectroscopy of human brain in vivo in the evaluation of multiple sclerosis: assessment of the load of disease. *Magn Reson Med* 1990;14:154–159
7. Nadler JV, Cooper JR. N-acetyl-L-aspartic acid content of human neural tumorous and bovine peripheral nervous tissues. *J Neurochem* 1971;178:313–319
8. Koller KJ, Zaczek R, Coyle J. N-acetyl-aspartyl-glutamate: regional levels in rat brain and the effects of brain lesions as determined by a new HPLC method. *J Neurochem* 1984;43:1136–1142
9. MacGowan JC, Schnall MD, Leigh JS. Magnetization transfer imaging with pulsed off-resonance saturation: variation in contrast with saturation duty cycle. *J Magn Reson Imaging* 1994;4:79–82
10. Marion D, Ikura M, Bax A. Improved solvent suppression in one- and two-dimentional NMR spectra by convolution of time-domain data. *J Magn Reson* 1989;84:425–430
11. Rose LM, Richards TL, Petersen R, Perterson J, Hruby S, Alvord EC. Remitting-relapsing EAE in nonhuman primates: a valid model of multiple sclerosis. *Clin Immunol Immunopathol* 1991;59:1–15
12. Matthews PM, Francis G, Antel J, Arnold DL. Proton magnetic resonance spectroscopy for metabolic characterization of plaques in multiple sclerosis. *Neurology* 1991;41:1251–1256
13. Miller DH, Austin SJ, Connelly A, Youl BD, Gadian DG, McDonald WI. Proton magnetic resonance spectroscopy of an acute and chronic lesion in multiple sclerosis. *Lancet* 1991;337:58–59
14. Van Hecke P, Marchal G, Johannik K, et al. Human brain proton localized NMR spectroscopy in multiple sclerosis. *Magn Reson Med* 1991;18:199–206
15. Narayana PA, Wolinsky JS, Jackson EF, McCarthy M. Proton MR spectroscopy of gadolinium-enhanced multiple sclerosis plaques. *J Magn Reson Imaging* 1992;2:263–270
16. Koopmans RA, Li DK, Zhu G, Allen PS, Penn A, Paty DW. Magnetic resonance spectroscopy of multiple sclerosis: in-vivo detection of myelin breakdown products. *Lancet* 1993;341:631–632
17. Davie CA, Hawkins CP, Barker GJ, et al. Detection of myelin breakdown products by proton magnetic resonance spectroscopy. *Lancet* 1993;341:630–631
18. Grossman RI, Lenkinski RE, Ramer KN, Gonzalez-Scarano F, Cohen JA. MR proton spectroscopy in multiple sclerosis. *AJNR Am J Neuroradiol* 1992;13:1535–1543
19. Birken DL, Oldendorf WH. N-acetyl-L-aspartic acid: a literature review of a compound prominent in ^{1}H-NMR spectroscopy studies of brain. *Neurosci Biobehav Rev* 1989;13:23–31
20. Loevner LA, Grossman RI, Cohen JA, Lexa FJ, Kessler D, Kolson DL. Microscopic disease in normal-appearing white matter on conventional MR images in patients with multiple sclerosis: assessment with magnetization-transfer measurements. *Radiology* 1995;196:511–515
21. Allen IV, Mckeown SR. A histological, histochemical and biochemical of the macroscopically normal white matter in multiplesclerosis. *J Neurol Sci* 1979;41:81–91
22. Brenner RE, Munro PMG, Williams SCR, et al. The proton NMR spectrum in acute EAE: the significance of the change in the Cho:Cr ratio. *Magn Reson Med* 1993;29:737–745
23. Hiehle JF, Lenkinski RE, Grossman RI, et al. Correlation of spectroscopy and magnetization transfer imaging in the evaluation of demyelinating lesions and normal appearing white matter in multiple sclerosis. *Magn Reson Med* 1994;32:285–293